Biochem. J. (2014) **464**, 3–11 (Printed in Great Britain) doi:10.1042/BJ20140778

The antimicrobial peptide LL-37 facilitates the formation of neutrophil extracellular traps

Ariane Neumann*, Evelien T. M. Berends†, Andreas Nerlich‡, E. Margo Molhoek§, Richard L. Gallo‖, Timo Meerloo¶, Victor Nizet**††, Hassan Y. Naim*[1] and Maren von Köckritz-Blickwede*[1]

*Department of Physiological Chemistry, University of Veterinary Medicine Hannover, 30559 Hannover, Germany
†Medical Microbiology, University Medical Center, 3584 CX Utrecht, The Netherlands
‡Institute of Microbiology, University of Veterinary Medicine Hannover, 30559 Hannover, Germany
§TNO Earth, Environmental and Life Sciences, Department CBRN protection, 2280 AA Rijswijk, The Netherlands
‖Division of Dermatology, Department of Medicine, University of California San Diego, San Diego, CA 92122, U.S.A.
¶Department of Cellular and Molecular Medicine, University of California San Diego, La Jolla, CA 92093, U.S.A.
**Department of Pediatrics, University of California San Diego, La Jolla, CA 92093, U.S.A.
††Skaggs School of Pharmacy and Pharmaceutical Sciences, University of California San Diego, La Jolla, CA 92093, U.S.A.

NETs (neutrophil extracellular traps) have been described as a fundamental innate immune defence mechanism. During formation of NETs, the nuclear membrane is disrupted by an as-yet unknown mechanism. In the present study we investigated the role of human cathelicidin LL-37 in nuclear membrane disruption and formation of NETs. Immunofluorescence microscopy revealed that 5 μM LL-37 significantly facilitated NET formation by primary human blood-derived neutrophils alone, in the presence of the classical chemical NET inducer PMA or in the presence of *Staphylococcus aureus*. Parallel assays with a random LL-37 fragment library indicated that the NET induction is mediated by the hydrophobic character of the peptide. The translocalization of LL-37 towards the nucleus and the disruption of the nuclear membrane were visualized using confocal fluorescence microscopy. In conclusion, the present study demonstrates a novel role for LL-37 in the formation of NETs.

Key words: cathelicidin, cell death, hydrophobicity, nuclear membrane, NETosis, neutrophil extracellular trap.

INTRODUCTION

The cell death mechanism 'NETosis' is a novel fundamental innate immune defence based on the specialized cell death of activated neutrophils, which release extracellular DNA fibres called NETs (neutrophil extracellular traps) with antimicrobial activity against several pathogens [1]. The underlying mechanisms leading to formation of NETs are incompletely understood. Importantly, NETosis differs from classical cell death mechanisms such as necrosis and apoptosis by evidence of disruption of the nuclear membrane, subsequent mixing of nuclear and granule components, and their combined release into the extracellular milieu of the cell [1]. The factors that are involved in damaging the nuclear membrane of mammalian cells during the process of NET formation are still not clear.

In contrast with the mammalian cellular membrane, the nuclear membrane contains low levels of cholesterol comparable with that observed in bacterial membranes [2]. The antimicrobial peptide LL-37, a member of the α-helical cathelicidins, binds and damages membranes deficient in cholesterol and sphingomyelin such as bacterial membranes [3]. LL-37 is produced by various different cell types, e.g. phagocytic leucocytes, cells of the mucosal epithelium and keratinocytes [4]. During inflammatory responses, the level of secreted LL-37 peptide level can dramatically increase [4,5] and the peptide can exert direct microbicidal activity against many bacteria, fungi and enveloped viruses. Furthermore, LL-37 has numerous immunomodulatory functions [4]. In the present study we hypothesized that LL-37 could potentially affect the nuclear membrane and thereby facilitate the formation of NETs by activated neutrophils.

MATERIALS AND METHODS

LL-37-dependent NET induction

Primary blood-derived neutrophils were isolated from fresh blood of healthy donors by density gradient centrifugation using Polymorphprep™ (Progen Biotechnik) as described previously [6]. The experiments were carried out in accordance with the declaration of Helsinki (2013) of the World Medical Association and have been approved by the Ethics Committee of the institution in which the work was performed. The content was obtained from each donor after full explanation of the purpose, nature and risk of all procedures used. The cells were seeded on to poly-L-lysine-coated glass slides in 24-well plates at a concentration of 5×10^5 cells/well (250 μl/well) or on 48-well plates at a concentration of 2×10^5 cells/well (100 μl/well). RPMI without Phenol Red (PAA) was used for cultivation of the cells at 37 °C and 5 % CO_2. Isolated neutrophils were incubated in the presence or absence of 25 nM PMA (Sigma) with 5 μM of LL-37 (Anaspec). In addition to full-length LL-37, a fragment library of eight different LL-37 fragments with overlapping sequences and various biochemical properties [7], a scrambled form of LL-37, hBD-3 (human β-defensin 3) and HNP-1 (human neutrophil peptide 1; Anaspec) at a concentration of 5 μM each as well as three concentrations of polymyxin B (0.5 μg/ml, 1 μg/ml and 2 μg/ml; Sigma), were used.

The stimulated cells were centrifuged for 5 min at 370 ***g*** and then incubated for the indicated time points at 37 °C with 5 % CO_2. PMA was used to trigger the formation of NETs in neutrophils [1,8,9]. After incubation the cells were fixed with 4 % PFA (paraformaldehyde) for 10 min at room temperature.

Abbreviations: cfu, colony-forming unit(s); hBD-3, human β-defensin 3; HNP-1, human neutrophil peptide 1; mCRAMP, mouse cathelicidin-related antimicrobial peptide; NA, numerical aperture; NET, neutrophil extracellular trap; PFA, paraformaldehyde.

[1] Correspondence may be addressed to either of these authors (email mkoeckbl@tiho-hannover.de or hassan.naim@tiho-hannover.de).

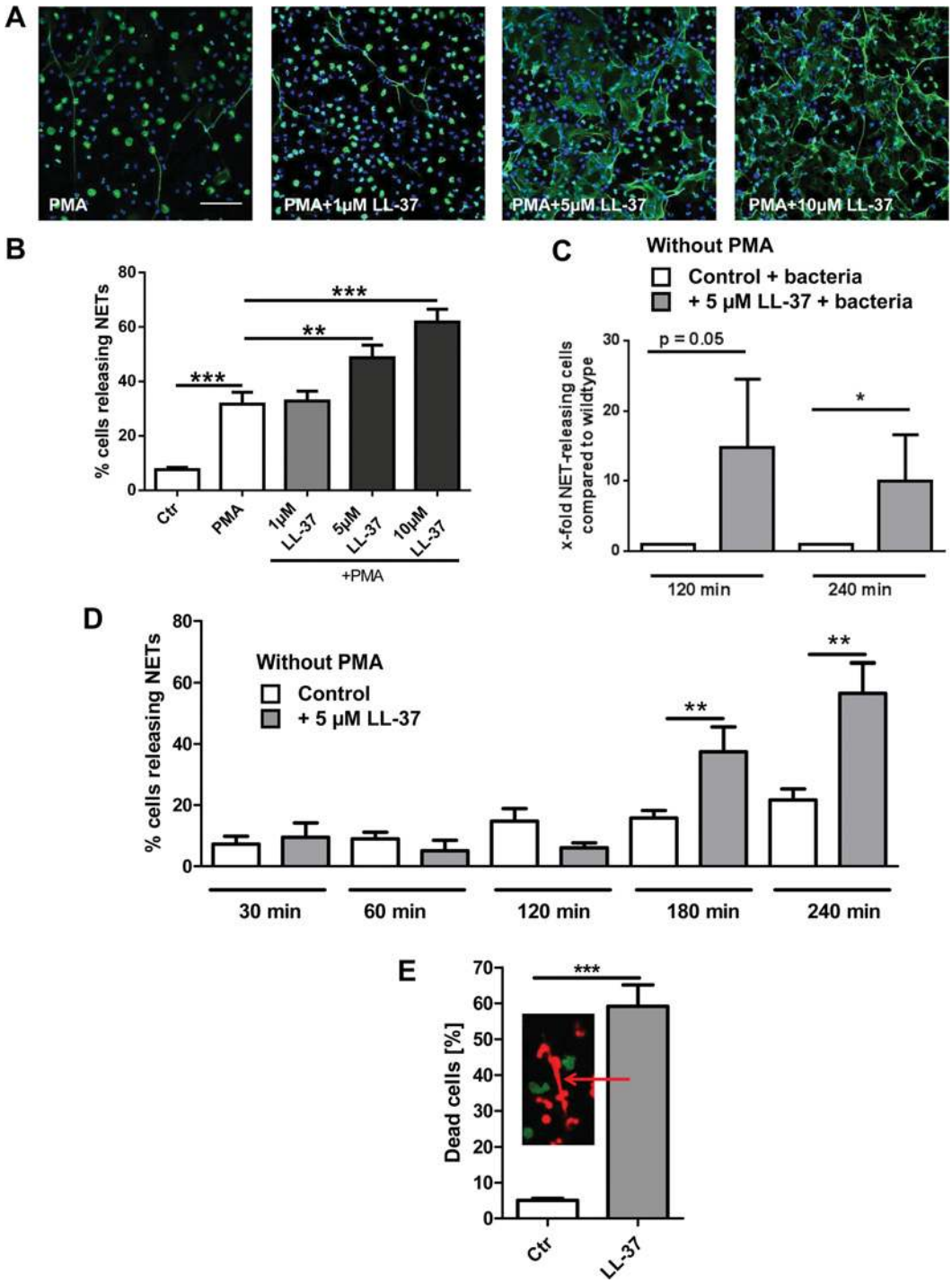

Figure 1 LL-37 facilitates the formation of NETs

Neutrophils derived from human blood were isolated by density gradient centrifugation and treated with 5 μM LL-37 in the presence or absence of 25 nM PMA or *S. aureus* USA 300. Formation of NETs was visualized using an Alexa Fluor® 488-labelled antibody against H2A–H2B–DNA complexes (green) in combination with DAPI to stain the nuclei in blue. (**A**) Representative fluorescent micrographs representing the results of the histogram in (**B**). Scale bar, 70 μm. (**B**) The percentage of cells releasing NETs in the presence or absence of 25 nM PMA for 2 h was quantified. (**C**) The percentage of *S. aureus*-infected cells releasing NETs in the presence or absence of 5 μM LL-37 was quantified. (**D**) The percentage of cells releasing NETs in the presence of 5 μM LL-37 (without PMA) was quantified over time. (**E**) Quantification of dead neutrophils in the presence or absence of LL-37 at 180 min of treatment. Note the release of DNA by dying neutrophils in the representative immunofluorescence shown within the histogram (red arrow). All histograms show the means ± S.E.M. of a minimum of 18 images derived from three independent experiments. $^{*}P < 0.05$, $^{**}P < 0.005$ and $^{***}P < 0.001$ by Student's *t* test.

Furthermore, cells were infected with *Staphylococcus aureus* USA 300 LAC strain (mid-exponential phase of growth) at a MOI (multiplicity of infection) of two bacteria per cell. Since LL-37 has direct antimicrobial activity against the bacteria, the surviving cfu (colony forming units) of the bacteria were quantified by plating aliquots of each sample on blood agar plates. Finally, the formation of NETs per 1×10^6 cfu was calculated.

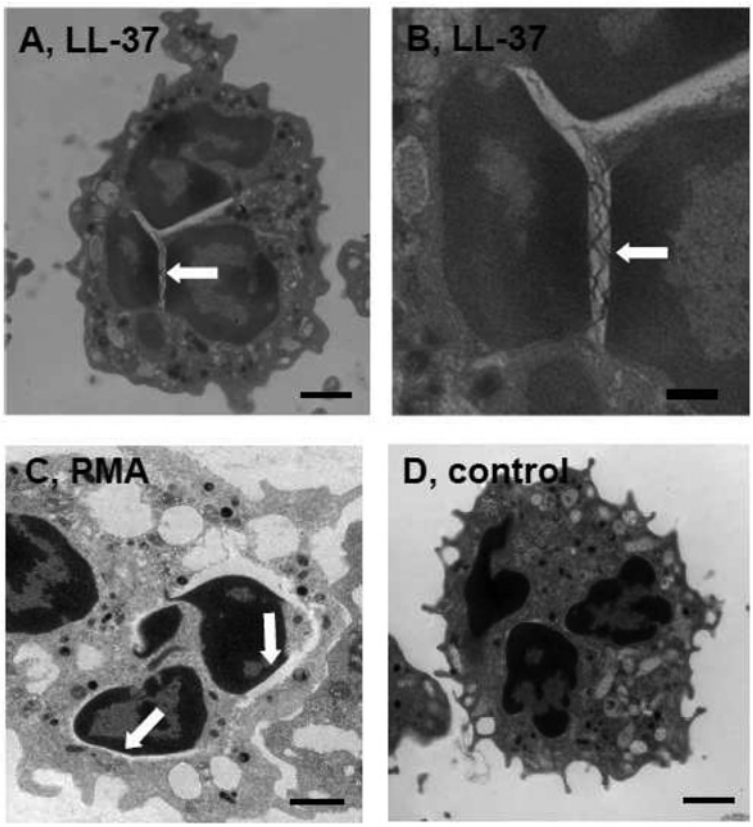

Figure 2 LL-37 leads to disruption of the nuclear membrane of neutrophils similar to that shown for the NET-inducing PMA positive control

Electron micrographs showing the disruption of the nuclear membrane of neutrophils during NET formation. Human blood-derived neutrophils were incubated for 2 h in RPMI plus 5 μM LL-37 (**A** and **B**), 25 nM PMA (**C**) or RPMI alone (**D**). In (**A**–**C**), the disruption of the nuclear membrane is visible (white arrows). Scale bars in (**A**) and (**C**), 1 μm; scale bar in (**D**), 0.35 μm; scale bar in (**B**), 0.75 μm.

Isolation of murine neutrophils

Male C57BL6/J mice (10 weeks old) were killed using isofluran and subsequent cervical dislocation. Legs were cut right before the hip joint and tissue and muscle were removed. Bone marrow from femur and tibia was flushed with HBSS (PAA) plus 1 % BSA (PAA) using a 26G cannula and cell strainer (100 μm; BD Falcon). Cells of four mice were pooled and centrifuged twice for 10 min at 370 ***g*** and 4 °C; pelleted erythrocytes were lysed with sterile water. For separation of suspension cells such as granulocytes from adherent monocytes, cells were incubated for 1 h at 37 °C with 5 % CO_2. The purity of isolated neutrophils was analysed by immunostaining using a FITC-labelled antibody against Ly6G (BD Pharmingen) or respective isotype control antibody (BD Pharmingen) to determine the percentage of neutrophils by flow cytometry and revealed 79.651 $\pm$ 3.015 % positive cells. A NET induction assay was performed as described above for human cells with 1×10^5 cells/well (100μl/well). All animal experiments were performed as required by the German regulations of the Society for Laboratory Animal Science (GV-SOLAS) and the European Health Law of the Federation of Laboratory Animal Science Associations (FELASA), and were approved by the local governmental animal care committees.

Visualization of NETs

Fixed cells were washed three times with PBS, permeabilized and blocked with 2 % BSA (Sigma) in 0.2 % Triton X-100 (Sigma)/PBS (PAA) for 45 min at room temperature. Incubation with a mouse monoclonal anti-H2A–H2B–DNA complex (clone PL2-6 [10], 0.5 μg/ml in 2 % BSA in 0.2 % Triton X-100/PBS) was carried out overnight at 4 °C, followed by washing (three times with PBS) and subsequent incubation with an Alexa Fluor® 488-labelled goat-anti-mouse antibody (Invitrogen) for 45 min at room temperature. After washing, slides were mounted in ProlongGold® antifade with DAPI (Invitrogen) and analysed by confocal fluorescence microscope using a Leica TCS SP5 confocal microscope with a 40×/0.75–1.25 HCX PL APO NA (numerical aperture) oil immersion objective. Settings were adjusted with control preparations using an isotype control antibody. Owing to donor-specific variations in spontaneous NET release, each experiment was performed with neutrophils derived from a minimum of three independent healthy blood donors. For each preparation, a minimum of five randomly selected images were acquired and used for quantification of NET-producing cells. Data were expressed as percentages of NET-forming cells in relation to the total number of cells visualized with DAPI to stain the nuclei.

Immunostaining of LL-37 and lamin-B-receptor

Immunostaining of LL-37 and lamin-B-receptor was performed using a similar immunostaining protocol as described above for the visualization of NETs. A polyclonal rabbit anti-LL-37 antibody was used at a final concentration of 1.6 μg/ml [11]. To visualize the nuclear membrane of cells, we used a monoclonal

A

Peptide	Sequence	Charge	% α-helicity	Cationicity	Hydrophobicity
LL-37	***LLGDFFRKSK EKIGKEFKRI VQRIKDFLRN LVPRTES***	6	68.6	100	***100.0***
LL-31	***LLGDFFRKSK EKIGKEFKRI VQRIKDFLRN L***	6	60.9	86.4	***101.3***
LL-25	LLGDFFRKSK EKIGKEFKRI VQRIK	6	65.8	63.1	69.1
LL-19	LLGDFFRKSK EKIGKEFKR	4	39.8	50.2	59.6
IG-25	IGKEFKRI VQRIKDFLRN LVPRTES	4	41.0	65.4	89.6
IG-19	***IGKEFKRI VQRIKDFLRN L***	4	32.7	60.7	***92.5***
RK-25	RKSK EKIGKEFKRI VQRIKDFLRN L	7	53.7	78.9	85.1
RK-19	RKSK EKIGKEFKRI VQRIK	7	25.5	67.8	52.6

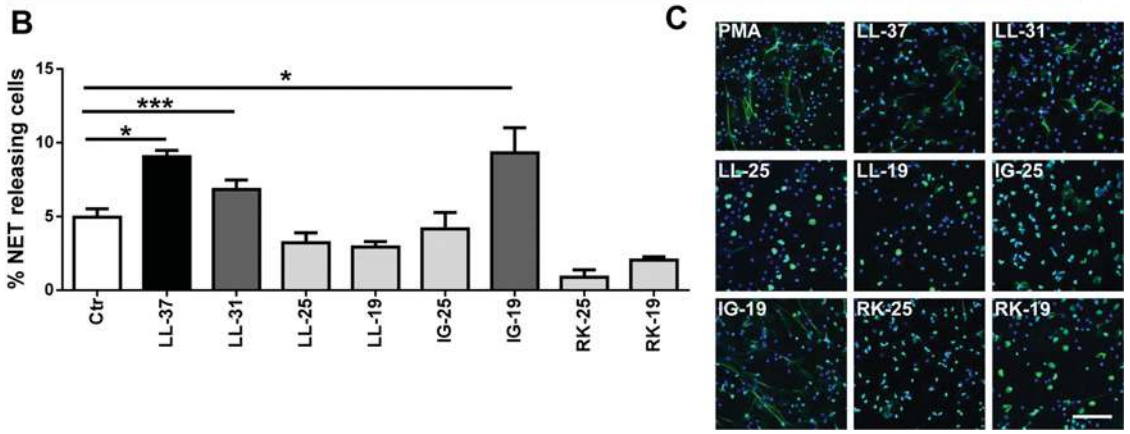

Figure 3 Hydrophobicity of LL-37 is associated with the LL-37-mediated NET formation as tested by a LL-37 fragment library

(**A**) Sequences and biochemical characteristics of LL-37 and the tested fragments. (**B**) Human blood-derived neutrophils treated with 5 μM LL-37 or LL-37 fragments in the presence of 25 nM PMA for 2 h. Formation of NETs was visualized using an Alexa Fluor® 488-labelled antibody against H2A–H2B–DNA complexes (green) in combination with DAPI to stain the nuclei blue. The percentage of cells releasing NETs was quantified. Besides LL-37, the fragments LL-31 and IG-19 were also able to augment the formation of NETs compared with PMA alone (Ctr). (**C**) Representative fluorescence micrographs showing the results of the histogram in (**B**). Scale bar, 100 μm. The histogram represents the means $\pm$ S.E.M. of a minimum of 18 images derived from three independent experiments. $^{*}P < 0.05$, $^{***}P < 0.001$ using Student's *t* test.

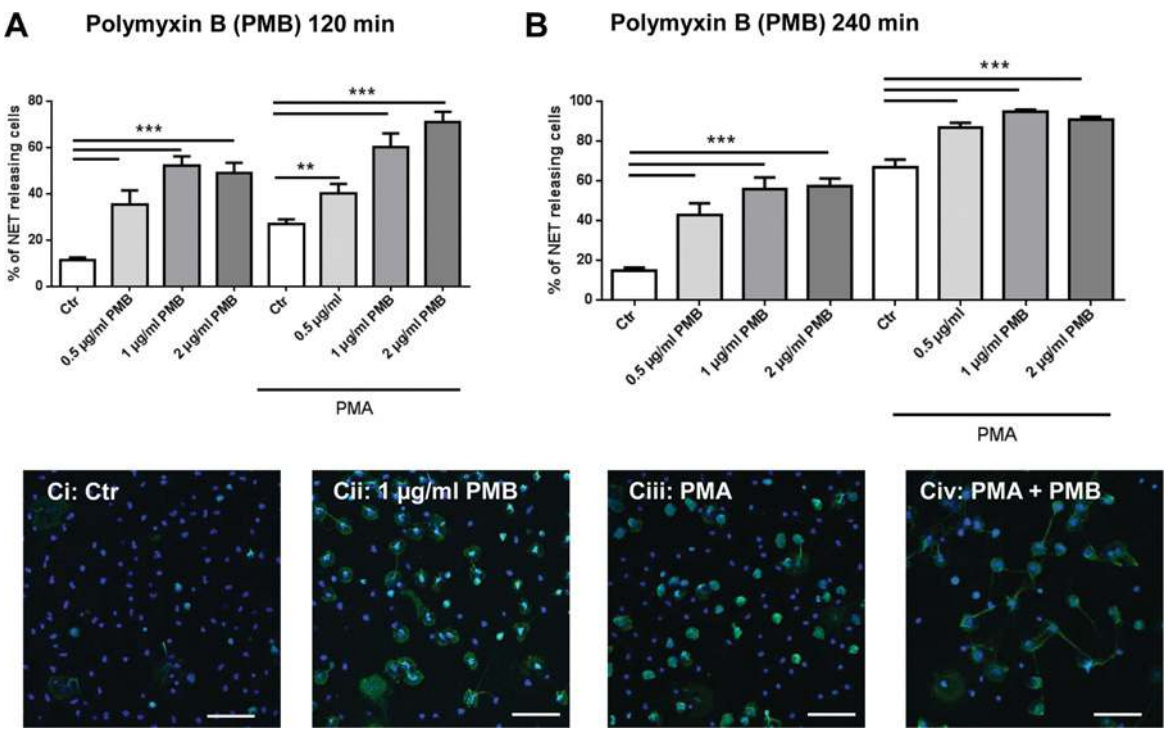

Figure 4 Polymyxin B induces NETs

(**A** and **B**) Human blood-derived neutrophils treated with 0.5, 1 or 2 μg/ml polymyxin B (PMB) in the absence or presence of 25 nM PMA for 2 h (**A**) or 4 h (**B**). Formation of NETs was visualized using an Alexa Fluor® 488-labelled antibody against H2A–H2B–DNA complexes (green) in combination with DAPI to stain the nuclei in blue. The percentage of cells releasing NETs was quantified. (**C**) Representative fluorescence micrographs showing the results of the histogram in (**A**). Scale bar, 70 μm. The histograms show the means $\pm$ S.E.M. of a minimum of 18 images derived from three independent experiments. $^{**}P < 0.005$, $^{***}P < 0.001$ by Student's *t* test.

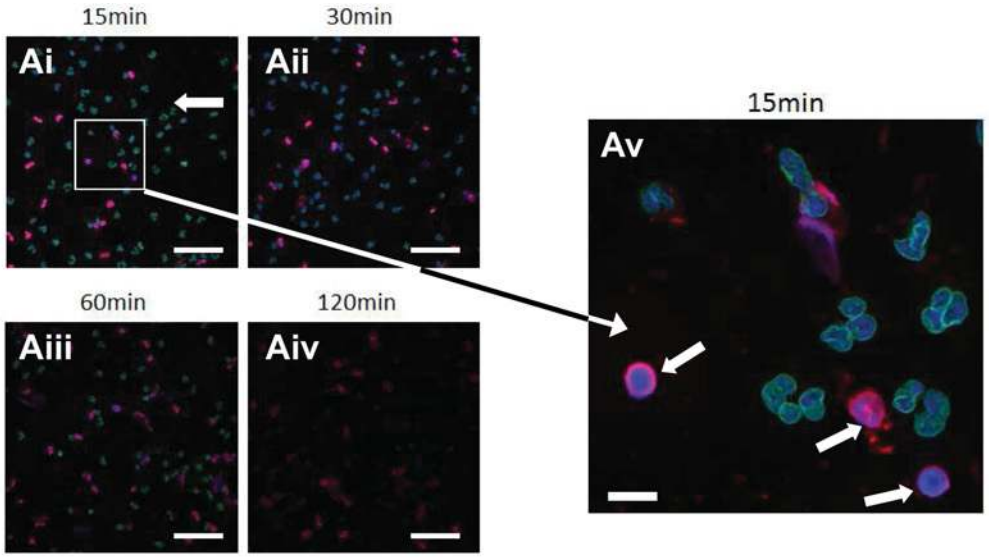

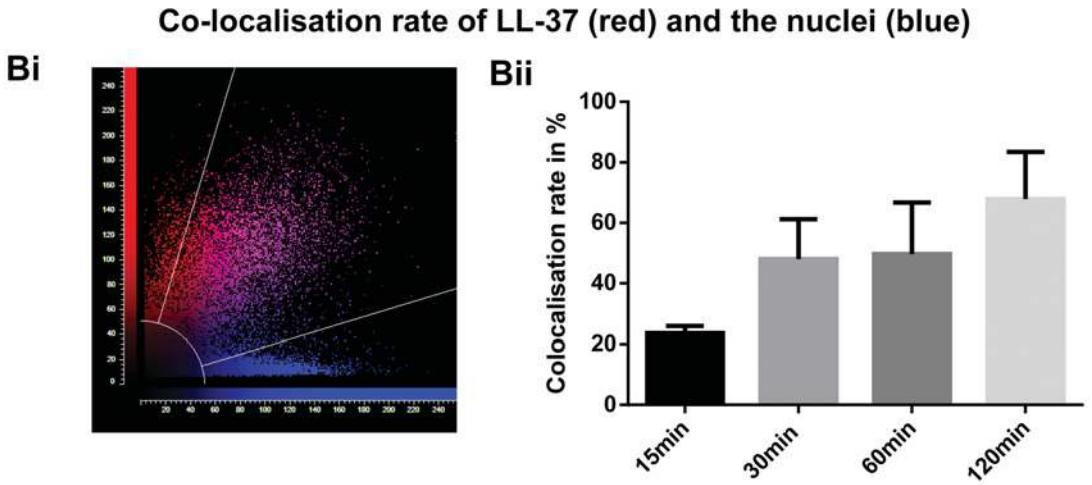

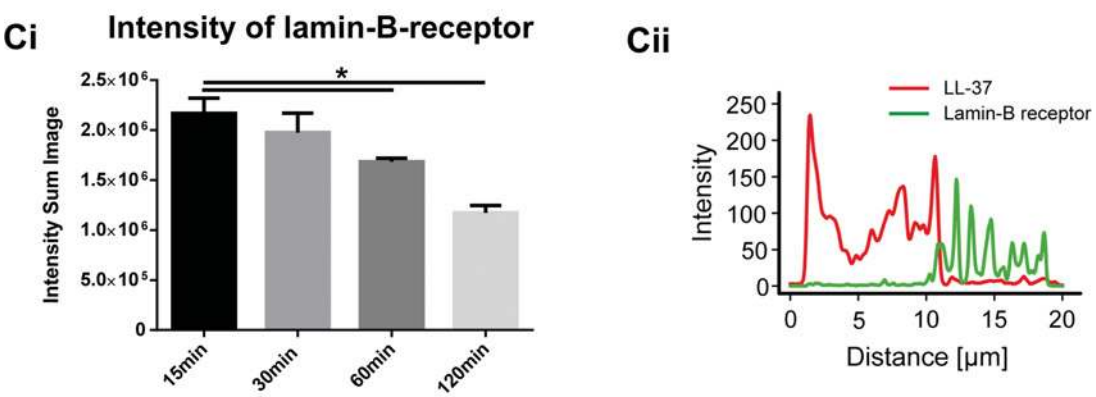

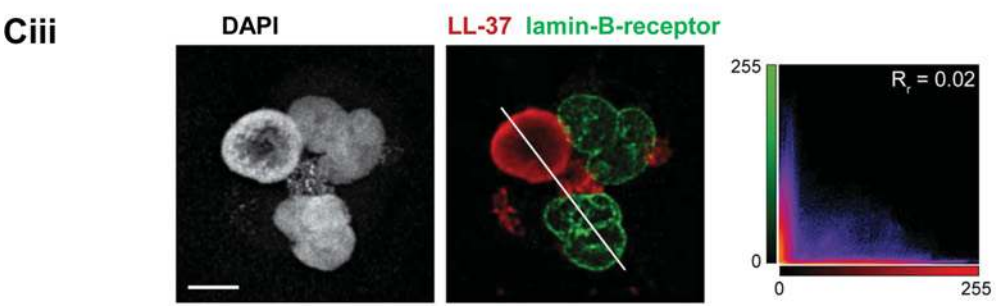

mouse anti-(lamin B receptor) antibody (0.33 mg/ml; 1:300 dilution; Abnova). Subsequently, samples were incubated with Alexa Fluor® 488 goat anti-mouse (1:1000 dilution; Invitrogen) and an Alexa Fluor® 633 goat anti-rabbit antibody (1:1000 dilution, Invitrogen). Mounted samples were examined using a TCS SP5 confocal laser-scanning microscope equipped with a 63×/1.4–0.6 NA HCX PL APO objective (Leica). Again, microscope settings were adjusted with control preparations using respective isotype control antibodies. Sum intensity of lamin B receptor and co-localization of LL-37 and DAPI was calculated with LAS-AF software (Leica).

Image stacks of typically 7.5 μm height with a *z*-distance of 0.125–0.17 μm per plane were acquired using 1 Airy unit pinhole diameter in sequential imaging mode to avoid bleed through. Image stacks were deconvolved using Huygens® Essential (Scientific Volume Imaging) and colour channels were aligned based on parameters determined from control measurements with 0.5 μm diameter TetraSpeck™ Microspheres (Life Technologies) performed under identical conditions. Co-localization of LL-37 and lamin B receptor was calculated with the Coloc 2 plugin in ImageJ/Fiji (http://fiji.sc/) on six focal planes from the middle of the cells. Maximum intensity projections were calculated for display purposes and adjusted for brightness and contrast using ImageJ/Fiji.

Electron microscopy

Human primary blood-derived neutrophils were isolated and treated as described above. Samples were immersed in modified Karnovsky's fixative (2.5 % glutaraldehyde and 2 % PFA in 0.15 M sodium cacodylate buffer, pH 7.4) for at least 4 h, post-fixed in 1 % osmium tetroxide in 0.15 M cacodylate buffer for 1 h and stained en bloc in 2 % uranyl acetate for 1 h. Samples were dehydrated in ethanol, embedded in epoxy resin, sectioned at 50–60 nm on a Leica UCT ultramicrotome, and picked up on Formvar and carbon-coated copper grids. Sections were stained with 2 % uranyl acetate for 5 min and Sato's lead stain for 1 min. Grids were viewed using a Tecnai G2 Spirit BioTWIN transmission electron microscope equipped with an Eagle 4k HS digital camera (FEI).

Quantification and visualization of cell death

For microscopic examination of cell death, cells were cultured on poly-L-lysine-coated glass coverslides and analysed for viability using the LIVE/DEAD viability/cytotoxicity kit for mammalian cells (Invitrogen) following the recommendations of the manufacturer.

Statistical analysis

Data were analysed using Excel 2003 (Microsoft) and GraphPad Prism 5.0 (GraphPad Software). All experiments were performed at least three times. NET experiments were performed with blood from a minimum of three different blood donors. Differences between the two groups were analysed using a one-tailed Student's *t* test. The significance is indicated as $*P < 0.05$, $**P < 0.005$ and $***P < 0.001$.

RESULTS AND DISCUSSION

LL-37 facilitates the formation of NETs

Different concentrations of LL-37 (1 μM, 5 μM and 10 μM) were used to stimulate primary blood-derived neutrophils in the presence of the neutrophil activator PMA (25 nM) for 2 h. The percentage of NET-releasing cells was calculated using immunofluorescence microscopy with an antibody directed against histone–DNA complexes (Figure 1A). As shown in Figures 1(A) and 1(B), a concentration of 5 and 10 μM LL-37 can significantly facilitate PMA-mediated NET formation.

LL-37 could also distinctly boost NET formation in the presence of *S. aureus* as a natural microbial stimulator for NETs after 2 and 4 h of co-incubation (Figure 1C). Interestingly, in the absence of PMA or *S. aureus*, LL-37 alone could also significantly induce NET formation at 3 or 4 h after treatment (Figure 1D) in association with death of the neutrophil (Figure 1E).

In accordance with the NETosis-associated typical phenotype [1], cells treated with LL-37 showed a clear disruption of the nuclear membrane by electron microscopy (Figures 2A and 2B), similar to cells treated with the potent NET stimulator PMA (Figure 2C). In contrast, non-stimulated control cells retained intact nuclear membranes (Figure 2D). Thus it might be assumed that LL-37-mediated NET formation is associated with the disruption of the nuclear membranes as previously described for NETosis [1].

Hydrophobicity is the essential characteristic responsible for mediating LL-37-induced NET formation

To characterize the biochemical properties involved in LL-37-dependent NET formation, NET induction experiments were performed using a fragment library of eight different LL-37 fragments with overlapping sequences and various biochemical properties (Figure 3A) [7]. Isolated neutrophils were stimulated with 25 nM PMA plus 5 μM of each different LL-37 peptide fragment, and the resulting percentage of NET-releasing cells was quantified. Besides the full-length LL-37 peptide, hydrophobic fragments LL-31 and IG-19 also enhanced NET formation by PMA-activated neutrophils (Figures 3B and 3C). A statistical analysis using Pearson correlation revealed that peptide hydrophobicity was associated with NET induction.

To support the hypothesis that the hydrophobic character of the peptide is associated with NET formation, the hydrophobic small molecule polymyxin B was additionally tested. Polymyxins, a group of cyclic cationic polypeptides originally derived from *Bacillus polymyxa*, share remarkable structural similarity with

Figure 5 LL-37 translocates to the nuclear membrane and leads to the removal of the lamin B receptor

(**A**) Fluorescence micrograph of a kinetic experiment, demonstrating the migration of externally added LL-37 (5 μM) to the nuclear membrane of human blood-derived neutrophils stimulated with 25 nM PMA (white arrows). The lamin B receptor as a marker for the nuclear membrane is visualized in green, LL-37 in red and the nuclei in blue. The scale bar in (**Ai**–**Aiv**) is 55 μm and the bar in (**Av**) is 8 μm. (**Bi**) Representative scatter plot of co-localization of LL-37 (red) and the nuclei (blue) at 120 min of treatment. (**Bii**) Co-localization rate of LL-37 (red) and the nuclei (blue). (**Ci**) Intensity of lamin B receptor (green) quantified using LAS-AF software (Leica). (**Cii** and **Ciii**). Maximum intensity projections of deconvolved confocal stacks, demonstrating the translocation of externally added LL-37 (5 μM) towards the nucleus. The nuclei stained with DAPI are shown in the left-hand panel of (**Ciii**). Lamin B receptor as a marker for the nuclear membrane is visualized in green and LL-37 in red (middle column). 2D scatter plots of voxel intensities in the red and green channels are shown in the right-hand panel. Pearson's correlation coefficient (*R*) was determined for voxel intensity correlation between the red and green channels using the Coloc 2 plugin in the ImageJ/Fiji software. Scale bar, 5 μm. The plot in (**Cii**) shows line profiles of the indicated region in (**Ciii**), illustrating that the lamin B receptor signal (green line) and LL-37 (red line) show no co-localization.

A

Peptide	Sequence	Charge
LL-37	LLGDFFRKSK EKIGKEFKRI VQRIKDFLRN LVPRTES	6
hBD-3	GIINTLQKYYCRVRGGRCAVLSCLPKEEQIGKCSTRGRKCCRRKK	11
HNP-1	ACYCRIPACIAGERRYGTCIYQGRLWAFCC	3
mCramp	GLLRKGGEKIGEKLKKIGQKIKNFFQKLVPQPEQ	6
Scr. LL-37	GLKLRFEFSKIKGEFLKTPEVRFRDIKLKDNRISVQR	6

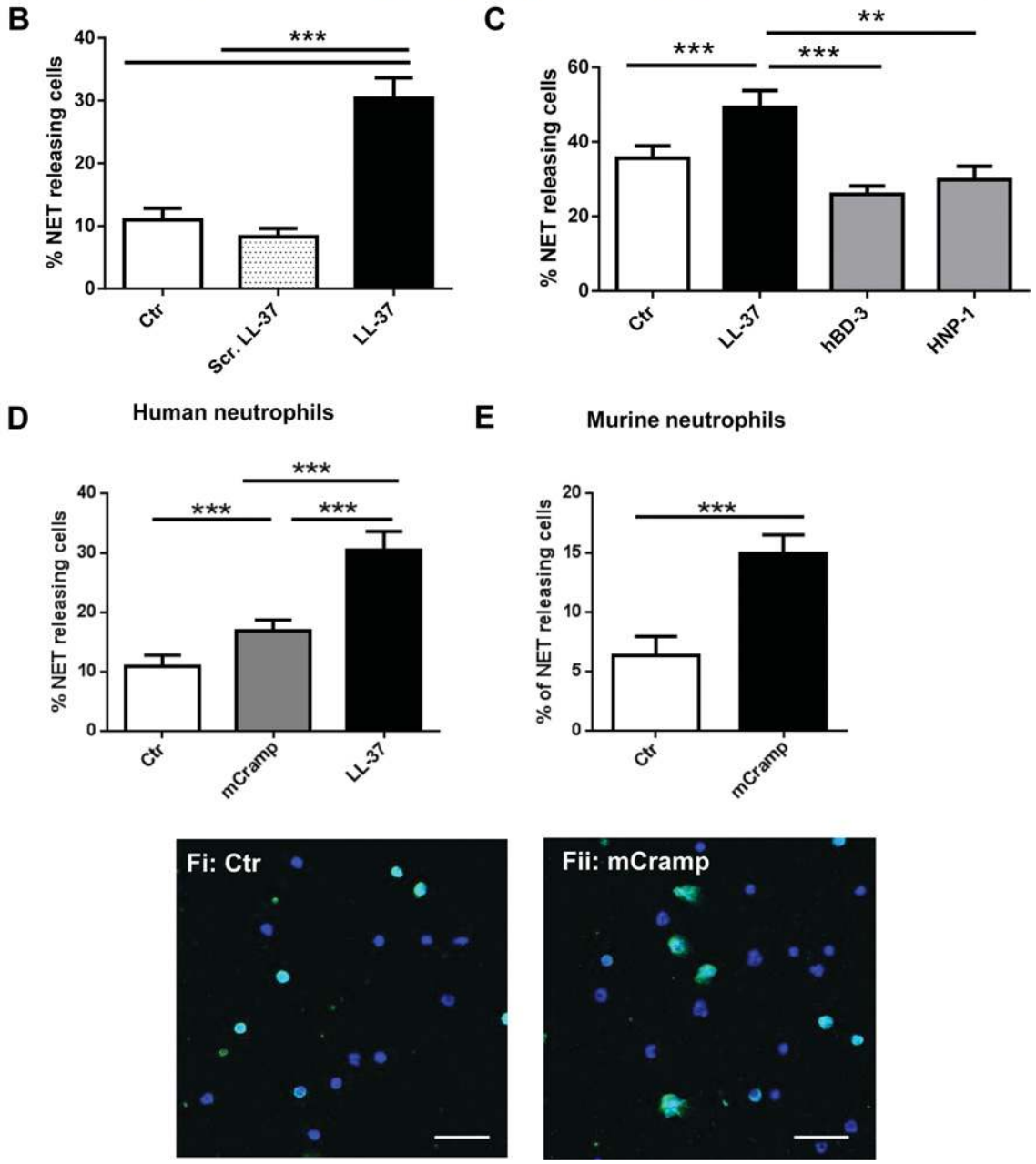

Figure 6 mCRAMP, but not hBD-3 and HNP-1 or a scrambled form of LL-37, facilitate NET formation

(**A**) Sequences of LL-37, scrambled LL-37, mCRAMP, hBD-3 and HNP-1. Neutrophils derived from human blood were isolated by density gradient centrifugation and treated with 5 μM of the respective peptide in the presence of 25 nM PMA. Formation of NETs was visualized using an Alexa Fluor® 488-labelled antibody against H2A–H2B–DNA complexes (green) in combination with DAPI to stain the nuclei in blue. (**B**) Percentage of cells releasing NETs of LL-37 wild-type or scrambled LL-37 compared with PMA alone (Ctr). (**C**) Percentage of cells releasing NETs comparing LL-37, hBD-3, HNP-1 and PMA alone (Ctr). (**D**) Percentage of cells releasing NETs comparing LL-37, mCRAMP and PMA alone (Ctr). The histograms show the means $\pm$ S.E.M. of a minimum of 18 images derived from three independent experiments. $^{**}P < 0.005$ and $^{***}P < 0.001$ by Student's *t* test. Furthermore murine neutrophils were isolated from the bone marrow of C57BL/6 mice and treated with 5 μM mCRAMP in the presence of 25 nM PMA for 2 h. (**E**) Percentage of cells releasing NETs was quantified compared with PMA alone (Ctr). The histogram is the means $\pm$ S.E.M. of 12 images derived from two independent mice. $^{***}P < 0.001$ by Student's *t* test. (**F**) Representative fluorescence micrographs showing the results of the histogram in (**E**). Scale bar, 25 μm.

cationic peptides. Cirioni et al. [12] stated that no statistically significant differences between LL-37 and polymyxin B were noted for antimicrobial and antiendotoxin activities in three different experimental rat models of Gram-negative sepsis. In the present study, similar to LL-37, the hydrophobic small molecule polymyxin B also showed a strong NET-inducing phenotype (Figure 4). A concentration of 0.5 μg/ml polymyxin B or higher (1 and 2 μg/ml) significantly facilitated the formation of NETs in human primary blood-derived neutrophils at 120 (Figure 4A) or 240 (Figure 4B) min of treatment in the presence or absence of PMA. Representative fluorescence micrographs are shown in Figure 4(C). These data support a model in which the hydrophobic character of the peptides is the key for the NET induction process of the antimicrobial peptide.

LL-37 mediates the disruption of the nuclear membrane during NET formation

The data from the peptide fragment analysis imply that LL-37-dependent NETosis is related to the hydrophobic character of the peptide which correlates with other studies showing that hydrophobicity of LL-37 is involved in binding and disruption of bacterial membranes [13]. Bacteria typically lack pathways for sterol production, but may incorporate cholesterol from their mammalian hosts [14]. A lower content of cholesterol and sphingomyelin in the membranes of bacterial cells makes them more susceptible to LL-37-mediated damage than mammalian cell membranes [3]. Where $\sim$2 μM LL-37 can disrupt bacterial membranes, $\sim$10 μM of peptide is required to damage cytoplasmic membranes of mammalian cells. However, the nuclear membrane contains lower levels of cholesterol compared with bacterial membranes [2]. We hypothesized that LL-37 could damage the nuclear membrane and facilitate NET formation by activated neutrophils. In *S. aureus*-infected lung tissue from a previous study [15], we found the mouse analogue of LL-37, namely mCRAMP (mouse cathelicidin-related antimicrobial peptide), surrounding DAPI-stained nuclei in neutrophils releasing NETs in response to intranasal infection with MRSA (methicillin-resistant *S. aureus*) strain USA 300. A kinetic approach to visualize localization of LL-37 in human neutrophils by immunofluorescence was undertaken with an antibody against the lamin B receptor as a marker for the nuclear membrane (Figure 5A; green). Over time, an increase in co-localization of LL-37 (red) with the nucleus stained with DAPI was detectable (Figure 5B), indicating a translocation of LL-37 towards the nucleus. At the same time the sum intensity of the lamin B receptor (green) decreased in parallel (Figure 5C), with almost no lamin B signal detectable after 2 h (Figure 5Aiv). Confocal microscopic investigations indicated that lamin B receptor and LL-37 show no co-localization as demonstrated by the scatter and line plots of Figures 5(Cii) and 5(Ciii). It may be hypothesized that LL-37 led to a damage of the nuclear membrane associated with the removal of the lamin B receptor.

mCRAMP facilitates NET formation in human neutrophils

Comparing the ability of LL-37 with a scrambled form of LL-37 and two other well-characterized hydrophobic human antimicrobial peptides (Figure 6A), hBD-3 and HNP-1, we found the NET-inducing effect to be specific for correctly folded LL-37 (Figures 6B and 6C). Neither the scrambled LL-37, hBD-3 nor HNP-1 induced enhanced NET formation (Figures 6B and 6C). However, mCRAMP also showed a significant NET-inducing effect in human as well as murine neutrophils (Figures 6D–6F), although significantly less compared with LL-37. These data indicate that the NET-inducing effect is not unique to human LL-37, but can be induced by other hydrophobic antimicrobial peptides. Interestingly, Kraemer et al. [16] showed that the human β-defensin 1 (but not β-defensin 3) was able to stimulate NET formation, but the underlying mechanism was not defined. Similar to what we have demonstrated for LL-37 in the present study, investigators have previously shown that β-defensin 1 could also be efficient in migrating to the nucleus [17].

In summary, in the present study we found that exogenous LL-37, at concentrations as low as 5 μM, translocates to the nucleus of neutrophils, leads to disruption of the nuclear membrane, and facilitates the formation of NETs. Such peptide concentrations are physiologically relevant as measured in the sputum of COPD (chronic obstructive pulmonary disease) patients [5]. Even higher concentrations are detectable in bronchoalveolar lavage fluid of infants with pulmonary or systemic infections (up to 300 μM) [18] or certain inflammatory skin conditions such as psoriasis (up to 1 mg/ml) [19].

Several cell types have been shown to release LL-37 in response to infection and inflammation, e.g. keratinocytes or epithelial cells as well as phagocytes [4]. Upon extracellular release soluble antimicrobial peptides, e.g. LL-37, can enter the host cells via endocytosis without damaging the cytoplasmic membrane [20]. Moreover, antimicrobial peptides have the well-known capacity to penetrate lipid bilayers and could enter the nuclear membrane by passive diffusion in an energy-independent manner [21]. On the basis of our findings, we presume that LL-37, released in substantial amounts, by e.g. epithelial cells or phagocytes upon infection, may contribute to disruption of the nuclear membrane and may thereby facilitate the formation of NETs during inflammatory and innate immune responses. Since the LL-37-mediated NET-inducing effect was most pronounced in the presence of an additional stimulation with PMA or *S. aureus*, it is likely that LL-37 acts in combination with other pathways of neutrophil activation, e.g. histone hypercitrullination by the PAD-4 (peptidyl-arginine-deiminase 4) [22,23] or histone degradation by elastase [24], to promote extensive release of NETs.

AUTHOR CONTRIBUTION

Ariane Neumann performed the research, analysed and interpreted data, and wrote the paper. Timo Meerloo designed, performed, analysed and interpreted the electron microscope studies. Evelien Berends performed research. Andreas Nerlich performed confocal co-localization studies. E. Margo Molhoek designed research with peptide fragments, provided peptide fragments and interpretation of the respective data. Richard Gallo, Victor Nizet and Hassan Naim provided critical design of the research and interpretation of data. Victor Nizet and Hassan Naim wrote the paper. Maren von Köckritz-Blickwede designed and performed research, analysed and interpreted data, and wrote the paper. All of the authors critically read the paper before submission.

ACKNOWLEDGEMENT

We thank Thomas Gutsmann, Research Center Borstel, Division of Biophysics, Germany, for helpful scientific discussions.

FUNDING

This work was supported in part by Deutsche Forschungsgemeinschaft [grant number KO 3552/4-1] and the National Institutes of Health [grant numbers AI052453 and AR052728 (to R.G. and V.N.)]. A.N. was supported by a fellowship from the Akademie für Tiergesundheit (AfT) e.V. and a fellowship from the Ph.D. program 'Animal and Zoonotic Infections' from the University of Veterinary Medicine Hannover.

REFERENCES

1 Fuchs, T. A., Abed, U., Goosmann, C., Hurwitz, R., Schulze, I., Wahn, V., Weinrauch, Y., Brinkmann, V. and Zychlinsky, A. (2007) Novel cell death program leads to neutrophil extracellular traps. J. Cell Biol. **176**, 231–241 CrossRef PubMed

2 van Meer, G., Voelker, D. R. and Feigenson, G. W. (2008) Membrane lipids: where they are and how they behave. Nat. Rev. Mol. Cell Biol. **9**, 112–124 CrossRef PubMed

3 Sood, R., Domanov, Y., Pietiäinen, M., Kontinen, V. P. and Kinnunen, P. K. (2008) Binding of LL-37 to model biomembranes: insight into target vs host cell recognition. Biochim. Biophys. Acta **1778**, 983–996 CrossRef PubMed

4 Nijnik, A. and Hancock, R. E. W. (2009) The roles of cathelicidin LL-37 in immune defences and novel clinical applications. Curr. Opin. Hematol. **16**, 41–47 CrossRef PubMed

5 Jiang, Y. Y., Xiao, W., Zhu, M. X., Yang, Z. H., Pan, X. J., Zhang, Y., Sun, C. C. and Xing, Y. (2012) The effect of human antibacterial peptide LL-37 in the pathogenesis of chronic obstructive pulmonary disease. Respir. Med. **106**, 1680–1689 CrossRef PubMed

6 von Köckritz-Blickwede, M., Chow, O., Ghochani, M. and Nizet, V. (2010) Visualization and functional evaluation of phagocyte extracellular traps. In Immunology of Infection. 3rd edition. Series: Methods in Microbiology (Kaufmann, S. and Kabelitz, D., eds), pp. 139–160, Academic Press, Elsevier Science, Maryland Heights, MO

7 Molhoek, E. M., den Hertog, A. L., de Vries, A. M., Nazmi, K., Veerman, E. C., Hartgers, F. C., Yazdanbakhsh, M., Bikker, F. J. and van der Kleij, D. (2009) Structure-function relationship of the human antimicrobial peptide LL-37 and LL-37 fragments in the modulation of TLR responses. Biol. Chem. **390**, 295–303 CrossRef PubMed

8 Brinkmann, V., Reichard, U., Goosmann, C., Fauler, B., Uhlemann, Y., Weiss, D. S., Weinrauch, Y. and Zychlinsky, A. (2004) Neutrophil extracellular traps kill bacteria. Science **303**, 1532–1535 CrossRef PubMed

9 von Köckritz-Blickwede, M. and Nizet, V. (2009) Innate immunity turned inside-out: antimicrobial defense by phagocyte extracellular traps. J. Mol. Med. **87**, 775–783 CrossRef PubMed

10 Losman, M. J., Fasy, T. M., Novick, K. E. and Monestier, M. (1992) Monoclonal autoantibodies to subnucleosomes from a MRL/Mp $(-)+/+$ mouse. Oligoclonality of the antibody response and recognition of a determinant composed of histones H2A, H2B, and DNA. J. Immunol. **148**, 1561–1569 PubMed

11 Dorschner, R. A., Pestonjamasp, V. K., Tamakuwala, S., Ohtake, T., Rudisill, J., Nizet, V., Agerberth, B., Gudmundsson, G. H. and Gallo, R. L. (2001) Cutaneous injury induces the release of cathelicidin anti-microbial peptides active against group A Streptococcus. J. Invest. Dermatol. **117**, 91–97 CrossRef PubMed

12 Cirioni, O., Giacometti, A., Ghiselli, R., Bergnach, C., Orlando, F., Silvestri, C., Mocchegiani, F., Licci, A., Skerlavaj, B., Rocchi, M. et al. (2006) LL-37 protects rats against lethal sepsis caused by gram-negative bacteria. Antimicrob. Agents Chemother. **50**, 1672–1679 CrossRef PubMed

13 Oren, Z., Lerman, J. C., Gudmundsson, G. H., Agerberth, B. and Shai, Y. (1999) Structure and organization of the human antimicrobial peptide LL-37 in phospholipid membranes: relevance to the molecular basis for its non-cell-selective activity. Biochem. J. **341**, 501–513 CrossRef PubMed

14 Razin, S. (1975) Cholesterol incorporation into bacterial membranes. J. Bacteriol. **124**, 570–572 PubMed

15 Berends, E. T., Horswill, A. R., Haste, N. M., Monestier, M., Nizet, V. and von Köckritz-Blickwede, M. (2010) Nuclease expression by *Staphylococcus aureus* facilitates escape from neutrophil extracellular traps. J. Innate Immun. **2**, 576–586 CrossRef PubMed

16 Kraemer, B. F., Campbell, R. A., Schwertz, H., Cody, M. J., Franks, Z., Tolley, N. D., Kahr, W. H. A., Lindemann, S., Seizer, P., Yost, C. C. et al. (2011) Novel anti-bacterial activities of β-defensin 1 in human platelets: suppresion of pathogen growth and signaling of neutrophil extracellular trap formation. PLoS Pathog. **7**, e1002355 CrossRef PubMed

17 Bick, R. J., Poindexter, B. J., Buja, L. M., Lawyer, C. H., Milner, S. M. and Bhat, S. (2007) Nuclear localization of HBD-1 in human keratinocytes. J. Burns Wounds **7**, e3 PubMed

18 Schaller-Bals, S., Schulze, A. and Bals, R. (2002) Increased levels of antimicrobial peptides in tracheal aspirates of newborn infants during infection. Am. J. Respir. Crit. Care Med. **165**, 992–995 CrossRef PubMed

19 Ong, P. Y., Ohtake, T., Brandt, C., Strickland, I., Boguniewicz, M., Ganz, T., Gallo, R. L. and Leung, D. Y. (2002) Endogenous antimicrobial peptides and skin infections in atopic dermatitis. N. Engl. J. Med. **347**, 1151–1160 CrossRef PubMed

20 Sandgren, S., Wittrup, A., Cheng, F., Jönsson, M., Eklund, E., Busch, S. and Belting, M. (2004) The human antimicrobial peptide LL-37 transfers extracellular DNA plasmid to the nuclear compartment of mammalian cells via lipid rafts and proteoglycan-dependent endocytosis. J. Biol. Chem. **279**, 17951–17956 CrossRef PubMed

21 Chan, Y. R. and Gallo, R. L. (1998) PR-39, a syndecan-inducing antimicrobial peptide, binds and affects p130. J. Biol. Chem. **273**, 28978–28958 CrossRef PubMed

22 Wang, Y., Li, M., Stadler, S., Correll, S., Li, P., Wang, D., Hayama, R., Leonelli, L., Han, H., Grigoryev, S. A. et al. (2009) Histone hypercitrullination mediates chromatin decondensation and neutrophil extracellular trap formation. J. Cell Biol. **184**, 205–213 CrossRef PubMed

23 Li, P., Li, M., Lindberg, M. R., Kennett, M. J., Xiong, N. and Wang, Y. (2010) PAD4 is essential for antibacterial innate immunity mediated by neutrophil extracellular traps. J. Exp. Med. **207**, 1853–1862 CrossRef PubMed

24 Papayannopoulos, V., Metzler, K. D., Hakkim, A. and Zychlinsky, A. (2010) Neutrophil elastase and myeloperoxidase regulate the formation of neutrophil extracellular traps. J. Cell Biol. **191**, 677–691 CrossRef PubMed

Received 23 June 2014/22 August 2014; accepted 2 September 2014
Published as BJ Immediate Publication 2 September 2014, doi:10.1042/BJ20140778